Kinetics of Iron Sulfide Formation in Aqueous Solutions

Nikolaos G. Harmandas and Petros G. Koutsoukos

Institute of Chemical Engineering and High Temperature Chemical Processes and
the Department of Chemical Engineering, University of Patras, P.O. Box 1414,
University Campus, GR 265 00 Patras, Greece

ABSTKACT

The formation of iron sulfides by spontaneous precipitation at 25 °C has been investigated in unstable supersaturated solutions by free-drift and constant supersaturation methods. In all cases an amorphous FeS was formed which in the presence of atmospheric oxygen in the solutions was partially converted to pyrite. The spontaneous precipitation of amorphous FeS was preceded by induction times inversely proportional to the solution supersaturation. The subsequent rates of precipitation were proportional to the solution supersaturation and showed a parabolic dependence on the relative supersaturation. At constant supersaturation and under a slight N_2 overpressure Mackinawite was identified as the initially forming phase with a plate-like and spherullitic morphology. The apparent order of the precipitation was found to be 1 which in connection with the results obtained from the free-drift experiments suggested a surface controlled *mechanism*.

KEYWORDS: Iron sulfide scale, Amorphous FeS, mackinawite, kinetics of formation supersaturation effect

INTRODUCTION

The tormation of scales composed of sparingly soluble salts is a serious impediment for the most efficient utilization of geothermal energy. The severity of the problem depends on the chemical nature of the solid deposits which in turn is determined by the chemical composition of the geothermal fluids. In several cases, geothermal brines may contain considerably high concentrations of hydrogen sulfide (Phillips *et al.*,1980). Upon contact of the geothermal fluids with metallic parts of the installations for the utilization of geothermal energy (lines, pumps etc.) corrosion may take place leading to iron dissolution and subsequent precipitation as iron sulfides which may form hard deposits. Moreover, additional dissolved iron may be present in the geothermal tluids originating from the interaction of water with the ores in the aquifer where the geothermal water is found. In all cases deposition of iron sulfides and corrosion are closely related. An efficient strategy aiming at the elimination of iron sulfide scale should focus in the thorough understanding of the conditions at which precipitation takes place. In this aspect the nature of the initially forming solid is also of paramount importance . For the iron sulfide system, a number of iron sulfides may be formed with various stoichiometries of Fe and S (Jellinek, 1968, Ward, 1970, Berner, 1964,1967, Power and Fine, 1976, Meyer *et al.*, 1958, Morse er *al.*,1987). A large number of factors determine the rate and the nature of iron sulfide precipitates and there is no agreement with respect to the mechanism of the formation of these solid phases (Cornwell and Morse, 1987, Schoonen and Barnes 1991a, b, c). In the present work we have attempted to identify the nature of the initially forming phases in an aqueous iron sulfide system and the tactors influencing this process. The experiments presented here were done in unstable supersaturated solutions and at conditions where: (i) The presence ot air was allowed and the solution supersaturation varied, (ii) The supersaturation was varied at constant pH. (iii) Supersaturation was kept constant and atmospheric air was excluded from the solution.

EXPERIMENTAL

A. Preparation of solutions

The working supersaturated solutions were prepared from stock solutions of the precipitating ions. Crystalline $(NH_4)_2Fe(SO_4)_2$ was used for the preparation of Fe(II) stock solutions and a 20% $(NH_4)_2S$ solution was used as a S(II) source. The former stock solution was used as a standard while the $(NH_4)_2S$ solution was standardized titrimetrically with dithizone indicator (Karabash, 1953, Charlot, 1974). Ammonium sulfate stock solutions to be used as supporting electrolyte for the adjustment of the ionic strength were prepared from the solid reagent. In all cases triply distilled deaerated water was used for the solution preparation.

B. Free drift experiments

Experiments were done in a thermostatted double walled Pyrex® glass vessel by mixing simultaneously equal volumes, 100 ml each of Fe(II) and S(II) solutions prepared from the respective stock solutions in the reactor which was magnetically stirred. The reaction vessel was sealed with a Perspex® lid with ports accommodating a combination glass / SCE electrode for pH measurements and a sampling port with a two way valve for the withdrawal of samples without disturbing the gas phase above the solution. The electrode was calibrated before and after each experiment with NBS buffer solutions (Bates, 1967). The free-drift experiments were done at:

(i) variable *pH*: Immediately following the preparation of the supersaturated solutions, the pH was neutral to slightly alkaline (7.00 - 7.40). Immediately a blackish color appeared and the solution pH drifted to more acidic values. The variation of pH was monitored by a pH meter connected with an x-t recorder. The reaction was followed until no further pH change was observed in the suspension. The time needed to reach this state of equilibrium depended on the solution supersaturation. The suspensions were filtered through membrane filters (0.2 μm) and the solid phase was dried overnight at 80 °C.

(ii) Controlled pH: The experiments were done as in (i). However, upon changes of the solution pH as small as 0.001 pH units, caused by the precipitation process, an automatic burette connected with a computer controlled titration system, shown in figure 1, added a solution of standard ammonium hydroxide and the pH was kept constant at the initial value set for each experiment (the precipitation of FeS results in pH drop).

The time interval between mixing of the iron and sultide solutions and the beginning of the addition of alkali titrant solution was taken as the induction time, i.e. the time needed for the first changes to be observed. Samples were withdrawn at various time intervals and filtered and the filtrates were analyzed for total iron by AA-spectroscopy (Perkin Elmer 305 A). The solids were kept in a dessicator in the absence of O_2 to

avoid oxidation of the sulfides formed. In all experiments the redox potential was monitored by a Pt/ SCE pair of electrodes.

C. Experiments at constant supersaturation

The supersaturated solutions were prepared as described before. The automatic titrating system used in the

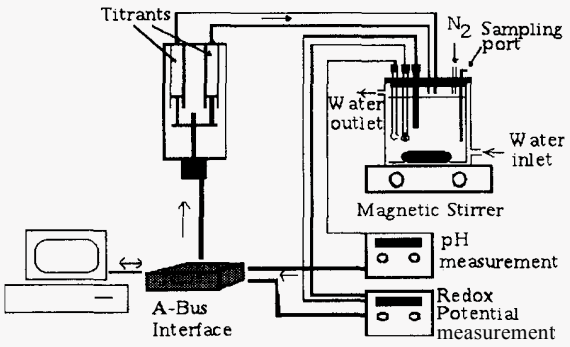

Figure 1: Computer controlled system for the control of various parameters (pH, redox potential solution supersaturation) for the precipitation of iron sulfides in supersaturated solutions.

pH stat experiments was in this case used with two syringes which added titrant solutions of $(NH_4)_2Fe(SO_4)_2$ and $(NH_4)_2S$ in a molar stoichiometric ratio of 1:1 corresponding to the precipitating solid. The titrant solutions in the two syringes were made as follows: From the previous experiments, it was assumed that the stoichiometry of the precipitating phase was Fe: S = 1: 1. If C_{Fe} is the total iron concentration (mol dm^{-3}) in the working solution and C_S the total sulfide concentration (mol dm^{-3}), while for the pH adjustment a total of C_B (mol dm-3) base solution was used, the solutions contained in the two burettes should be:

Burette 1: $FC_{Fe} + 2C_{Fe} = C_{Fe}(F+2)$ M of $(NH_4)_2Fe(SO_4)_2$
Burette 2: $FC_S + 2C_S = C_S(F+2)$ M of $(NH_4)_2S$
$+ \; 2C_B$ M of NH_4OH

Where F is an arbitrary constant (in our experiments it varied from 15 to 50 depending on the rate of precipitation). It is obvious therefore that F mol dm^{-3} of $(NH_4)_2SO_4$ should be added in the working solution to avoid dilution. As may be seen from the above calculations an error in the estimates of the titrant solutions (e.g. by assuming the wrong stoichiometry for the precipitating solid) would result in change of the solution supersaturation as the precipitation process is progressing. In order to verify the fact that through the titrant addition the solution supersaturation was kept constant, samples were withdrawn at various times, filtered through membrane filters and the filtrates were analyzed for iron. Sulfur analysis was not done since the concentrations analyzed were below the analytical limit of the method employed (1×10^{-4} M). The solids collected on the filters were kept in an inert atmosphere to avoid solid phase oxidation and they were examined by powder x-ray diffraction ,scanning electron microscopy and FT- IR . The rates of precipitation were obtained from plots of the volume ot the titrants added as a function of time. The curve obtained was fitted to a polynomial and the derivative at t=O was taken as the initial rate of precipitation of iron sulfide.

RESULTS AND DISCUSSION

The driving force for the precipitation of iron sulfide, FeS in aqueous supersaturated solutions is the difference in chemical potentials corresponding to the equilibrium, μ_∞, and the supersaturated solutions, μ_s, respectively i.e.

$$\Delta\mu = \mu_\infty - \mu_s$$
$$= \{\mu^o_\infty + kT\ln(\alpha_{Fe^{2+}}\alpha_{S^{2-}})^{1/2}_\infty\} - \{\mu^o_s + kT\ln(\alpha_{Fe^{2+}}\alpha_{S^{2-}})^{1/2}_s\}$$

assuming that $\mu^o_\infty = \mu^o_s$

$$\Delta\mu = -kT\ln\frac{(\alpha_{Fe^{2+}}\alpha_{S^{2-}})^{1/2}_s}{(\alpha_{Fe^{2+}}\alpha_{S^{2-}})^{1/2}_\infty}$$

or

$$\Delta\mu = -\frac{kT}{2}\ln\Omega \qquad (1)$$

In eq. (1) **k**, T are the Boltzmann constant and the absolute temperature respectively and

$$\Omega = \frac{\alpha_{Fe^{2+}}\alpha_{S^{2-}}}{K^o_{S,FeS}} \qquad (2)$$

with $K^o_{S,FeS}$ the thermodynamic solubility product of FeS. The relative solution supersaturation for FeS is defined as:

$$\sigma_{FeS} = \Omega^{1/2} - 1 \qquad (3)$$

It is obvious therefore that the knowledge ot the solution speciation is needed for the calculation of the solution supersaturation. The computation was done taking into account the equilibria and the corresponding constants summarized in Table 1, the mass balance equations for total iron and

Table 1: Aqueous equilibria for the computation of solution speciation in Fe(II) -H_2S - $(NH_4)_2SO_4$ - H20 systems

Equilibrium			logK°	ref
$H_2S(g)$	⇔	$H_2S(aq)$	0.99	a
$HS^- + H^+$	⇔	H_2S (aq)	7.02	a
$S^{2-} + H^+$	⇔	HS^-	13.90	a
$NH3 + H^+$	⇔	NH_4^+	9.24	a
$SO_4^{2-} + H^+$	⇔	HSO_4^-	1.99	a
$Fe^{2+} + SO_4^{2-}$	⇔	$FeSO_4^\circ$	2.20	a
$Fe^{2+} + OH^-$	⇔	$FeOH^+$	4.50	a
$Fe^{2+} + 2OH^-$	⇔	$Fe(OH)_2^\circ$	7.40	a
$Fe^{2+} + 3OH^-$	⇔	$Fe(OH)_3^-$	10.00	a
$Fe^{2+} + 4OH^-$	⇔	$Fe(OH)_4^{2-}$	9.60	a
$Fe^{2+} + 2H^+ + 2S^{2-}$	⇔	$Fe(HS)_2$	36.75	b

a: Smith and Martell, 1976
b: Naumov *et al.*,1974

Table 2. Thermodynamic solubility products of the various iron sulfides forming in aqueous media

Name	Formula	Expression		Ref.
Amorphous	FeS	$\alpha_{Fe^{2+}}\alpha_{S^2}$	1.437×10^{-17}	a
Troilite	a-FeS	$\alpha_{Fe^{2+}}\alpha_{S^2}$	6.17×10^{-17}	b
Pyrrhotite	$Fe_{0.98}S$	$\alpha_{Fe^{2+}}\alpha_{S^{2-}}$	2.70×10^{-19}	b
Mackinawite	FeS	$\alpha_{Fe^{2+}}\alpha_{S^{2-}}$	2.88×10^{-18}	c,d
Greigite	Fe_3S_4	$\alpha^3_{Fe^{2-}}\alpha^4_{S^{2-}}$	2.99×10^{-55}	a
Pyrite	FeS_2	$\alpha_{Fe^{2+}}\alpha^2_{S^{2-}}$	5.01×10^{-31}	a
Marcasite	FeS_2	$\alpha_{Fe^{2+}}\alpha^2_{S^{2-}}$	5.62×10^{-31}	a

a: Morse et al., 1987
b: Schoonen and Barnes,1991a
c: Berner, 1967
d: Morse and Arakaki, 1993

total sulfide and the charge balance using the HYDRAQL code (Papelis *et al.*,1988). The solution supersaturation was calculated with respect to all iron sulfides shown in Table 2.

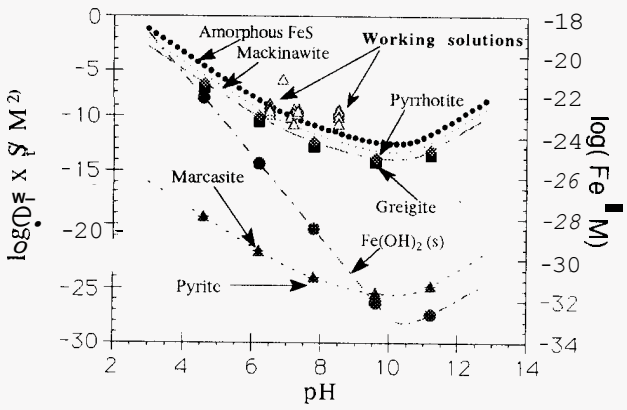

Figure 2: Solubility isotherms of iron sulfides and $Fe(OH)_2(s)$ with the conditions of the supersaturated solutions used in the present work.

However. from the free-drift experiments the solid phase forming was amorphous to x-ray diffraction and the kinetics analysis was done with respect to this phase. It should be noted that this phase was also formed in free-drift spontaneous precipitation at high pH (8.27 - 8.790) 0.4 M NaCl and 25° C. The experimental conditions used in the present work are shown in Figure 2. In this thermodynamic diagram as may be seen a number of experiments (those corresponding to the free-drift) are supersaturated with respect to the amorphous FeS which is obviously stabilized kinetically. The induction times were inversely proportional to the solution supersaturation as may be seen in Figure 3. As may be seen the labile zone at the iron sulfide system is rather narrow and is confined in very low total iron (Fe_t) analytical concentrations. According to the classical nucleation theory a linear relationship exists between the logarithm of the induction times, $\log t_{ind}$, and $(\log\Omega)^{-2}$ (Mullin,1993). According to this fomalism the plots obtained consisted of two linear branches with different slopes as may be seen in figure 4.

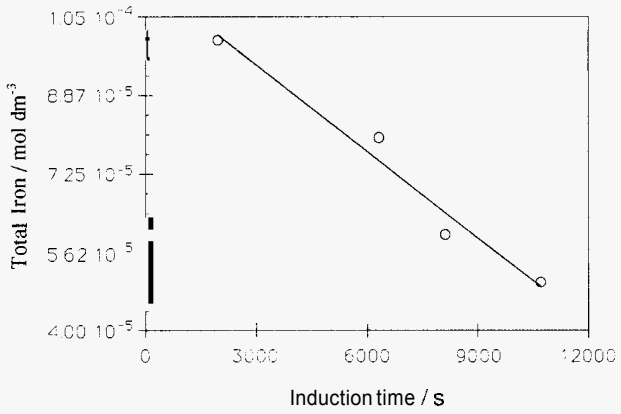

Figure 3: Dependence of the induction times measured for the spontaneous precipitation of amorphous FeS by free-drift experiments; 25° C.

The change in slope was observed at a supersaturation threshold of Ω_{am}= 37, which may be seen as a point marking a division between homogeneous and heterogeneous nucleation. Similar plots have been reported for $CaCO_3$ (Sohnel and Mullin, 1978) and for nickel ammonium sulfate (Mullin and Ang, 1976). From the slopes of the two parts, values of 81 and 206 mJ m^{-2} respectively were calculated for the surface energy of the nucleating phase, The high value of 206 mJ m^{-2} obtained for the homogeneous precipitation region, is within the order of magnitude anticipated according to the classical nucleation theory.

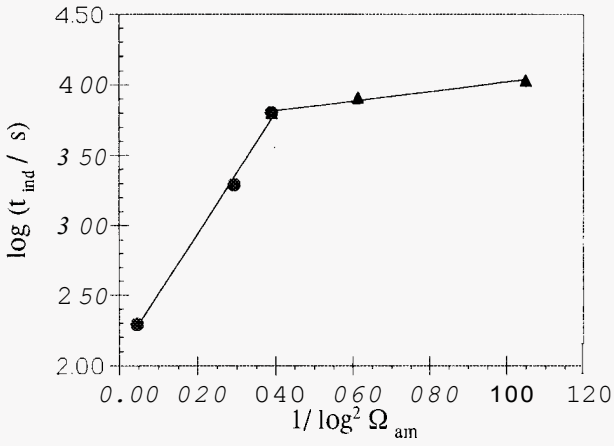

Figure 4: Dependence of the induction time on the relative solution supersaturation for amorphous FeS in free-drift experiments according to the classical nucleation theory, 25 °C.

Further mechanistic information was obtained by experiments done at sustained solution supersaturation since the rapid solution desupersaturation may change the nature of the crystalline phase forming. The experimental conditions of these experiments are summarized in table 3.

Table 3: Precipitation of Mackinawite in aqueous solutions at conditions of sustained solution supersaturation 25 "C

Exp. #	$Fe_t = S_t$ / x 10^{-5} M	Inert Electrolyte* x 10^{-3} M	pH	Ω_{mack}	Rate / x 10^{-9} mole FeS s^{-1}
53	1.0	0.3	7.19	3.11	1.2
55	2.0	0.6	7.10	8.07	2.8
56	3.0	0.9	7.30	24.20	6.6
57	4.0	1.2	7.32	37.00	7.9
50	5.0	3.0	7.36	47.2	12.6

+ Prepared from $(NH_4)_2Fe(SO_4)_2$ and $(NH_4)_2$.

* In all cases $(NH_4)_2SO_4$ was used for the ionic strength adjustment.

The rates of precipitation measured as may be seen in Table 1, were proportional to the solution supersaturation. The concentrations were chosen so that in all experiments, the solutions were supersaturated with respect to amorphous FeS and Mackinawite. The solid collected showed the three most characteristic Mackinawite peaks as may be seen in the x-ray diffractogram in figure Sa. Upon exposure to atmospheric oxygen for 24 hours the sulfide was converted to Fe(II) oxide, lepidocrocite (figure Sb). During the course of precipitation there has been a shift to larger particle sizes, while smaller particles were reduced probably through a crystal ripening mechanism occurring simultaneously with the precipitation process. In figure 6 the particle number and their size distribution with time is presented for lower supersaturations (a) and higher supersaturations (b). In the latter case it is obvious that the size distribution is rather broad and may be attributed to enhanced aggregation because of the faster rate of production of secondary nuclei at high supersaturation.

The kinetics analysis of crystal growth of Mackinawite was done according to the semiempirical expression

$$\text{Rate} = \frac{dm}{dt} = Ko'' \qquad (4)$$

where K is a rate constant depending on the active growth sites and n the apparent reaction order. The fit according to eq. (4), of the logarithm of the rates as a function of the relative

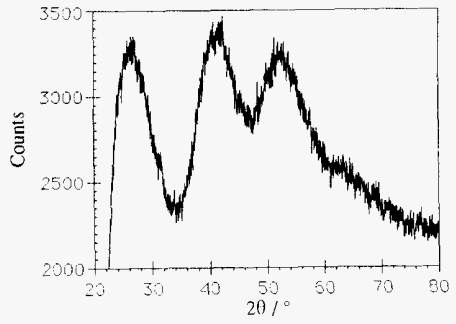

a

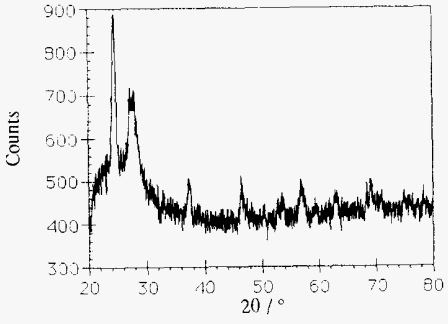

b

Figure 5: Powder x-ray diffractograms of : a. Spontaneously precipitated Mackinawite, b. Mackinawite converted to lepidocrocite by oxidation after exposure to the atmospheric oxygen.

solution supersaturation was satisfactory, as may be seen in figure 7 and gave a value of n=1.

The first order dependence of the rates on the relative solution supersaturation suggested that the rate determining process is the integration of the cations into the kinks from a layer adjacent to the crystal surface (Sohnel and Garside, 1992). The value of $5x10^{-10}$ obtained from the intercept of the straight line in figure 7 for the rate constant K compares well with the values of a number of sparingly soluble salts (Sohnel and Garside, 1992). It should be noted that the electron microscopic analysis showed that the amorphous solid consisted of granular crystallites (<0.1 μm) while Mackinawite had the same granular morphology but the crystallites were aggregated in plate-like formations. In all cases the solid phase showed formation of aggregates, fact explaining the relatively large sizes shown in the particle size distribution profiles. The power law described by eq. **4** was also used to analyze the kinetics results from the free-drift experiments where amorphous FeS was formed. In this case a parabolic law was found (i.e. n=2) which suggested the same, surface controlled mechanism,

CONCLUSIONS

The precipitation characteristics of iron sulfide depend on the solution supersaturation. At high supersaturations amorphous FeS is formed and a supersaturation ratio of ca. $4x10^{15}$ is the threshold for homogeneous nucleation. The growth at sustained solution supersaturation suggested that it is possible to precipitate directly Mackinawite from aqueous solutions which if exposed to atmospheric oxygen converts to iron oxides. The formation of Mackinawite is a surface diffusion controlled process.

Acknowledgment: A grant from the commission of the European Union JOU-CT92-0108 in support of this work is gratefully acknowledged.

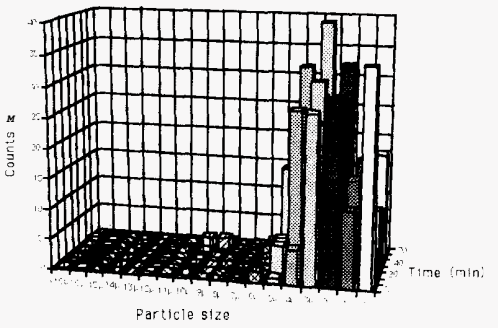

a

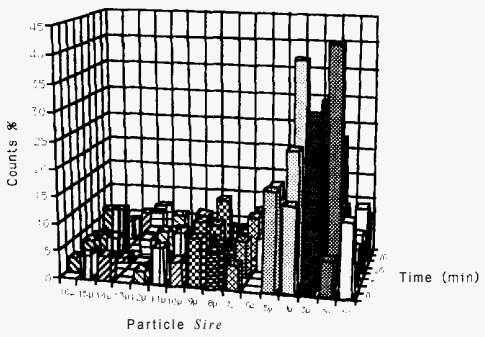

b

Figure 6: Particle number and particle size distribution as a function of time for the precipitation of Mackinawite at constant solution supersaturation, 25 "C: a. Low supersaturation, b. High supersaturation.

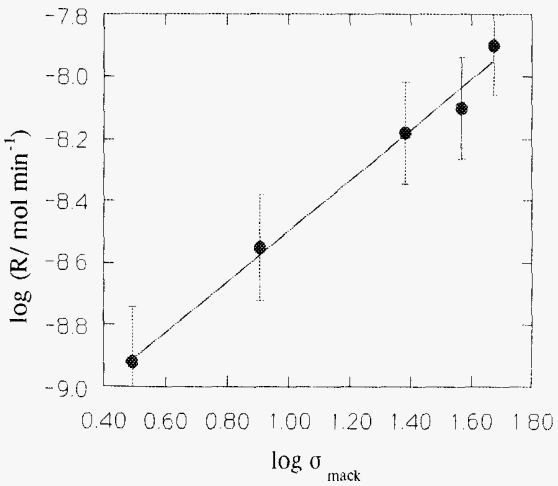

Figure 7: Kinetics plot for the precipitation of Mackinawite at constant solution supersaturation; 25 °C.

REFERENCES

Bates, R.G., (1967). *Determination of pH*, J. Wiley, New York. 479 pp.

Berner, R.A., (1964). Iron sulfides formed from aqueous solutions at low temperatures and atmospheric pressure. *J. Geol.*, Vol. 72, pp 293 - 306.

Berner R.A.. (1967). Thermodynamic stability of sedimentary iron sulfides. *Amer. J. Science,* Vol. 265, pp 773 - 785.

Charlot, G., (1974), *Chimie Analytique Quantitative*, Masson **Ed.**, 6eme Ed. 571 pp.

Cornwell J.C., Morse, J.W., (1987). The characterization of iron sulfide minerals in anoxic marine sediments. *Marine Chem.*, Vol. 22, pp 193 - 206.

Jellinek, F., (1968), *Inorganic Sulfur* Chemistry, Elsevier, Amsterdam, 715 pp.

Karabash, A.G., (1953). Use of dithizone as extraction indicator. *Zhur. Anal. Khim.*, Vol. 8(140), pp 140-151.

Meyer. F.H. , Riggs, O.L., McGlasson P.L., Sudberry, J.D., (1958). Corrosion of mild steel in H_2S environments. *Corrosion*, Vol. 14, pp.109 - 113.

Morse, J.W., Arakaki, T., (1993). Adsorption and coprecipitation of divalent metals with mackinawite (FeS). *Geochim. Cosmochim. Acta,* Vol. 57, pp. 3635 - 3640.

Morse, J.W., Millero F.J., Cornwell J.C., Rickard, D., (1987). The chemistry of the hydrogen sulfide and iron sulfide systems in natural waters. *Earth Science* Review, Vol. 24, pp 1 - 42.

Mullin, J.W., (1993). *Crystallization.* 3rd Ed., Butterworth - Heinemann, Oxford, pp. 172-201.

Mullin, J.W., Ang, H.M.. (1976). Nucleation characteristics of aqueous nickel ammonium sulphate solutions. *Faraday* Society *Discussions,* Vol. 61, pp 141- 148.

Naumov, G.B., Ryzhenko B.N., Khodashovski I.L., (1974). *Handbook of Thermodynamic Data.* US Geol. Survey WRD-74-001, NTIS PB-226 722/ AS.

Papelis, C., Hayes, K.F., Leckie. J.O. (1988). *HYDRAQL: A program for the Computation of Chemical Equilibrium Composition of Aqueous Batch Systems Including Surface Complexation Modeling of Ion Adsorption at the Oxide / Solution Interface.*, Tech. Report No 306, Stanford University, Stanford CA. 130 pp.

Phillips, S.L., Mathus, A.K., Garrison W., (1980). *Treatment Methods for Geothermal Brines*, Special Technical Publication 717, ASTM, Washington D.C. 207 pp.

Power, L.F. , Fine, H.A., (1976). The iron-sulfur system. Part 1. The structures and physical properties of the compounds of the low-temperature phase fields. *Minerals Sci. Eng.*, Vol. 8, pp 106 - 112.

Schoonen, M.A.A., Barnes, H.L. (1991a). Reactions forming pyrite and marcasite from solution: I. Nucleation of FeS_2 below 100 °C. *Geochim. Cosmochim. Acta.* Vol. 55, pp. 1495 - 1504.

Schoonen, M.A.A. Barnes, H.L., (1991b). Reactions forming pyrite and marcasite from solution: II. Via FeS precursors below 100 °C. *Geochini. Cosmochim. Acta*, Vol. 55 pp.1505 - 1514.

Schoonen, M.A.A. Barnes, H.L., (1991c). Mechanisms of pyrite and marcasite formation from solution: III. Hydrothermal Processes. *Geochim. Cosmochim. Acta,* Vol. 55, pp 3491 - 3504.

Smith, R.M., Martell, A.E., (1976). *Critical Stability Constants V.4 - Inorganic complexes* , Plenum Press. New York + London. 257 pp.

Sohnel, O., Garside, J.,(1992). *Precipitation*, Butterworth - Heinemann, Oxford, pp 92-96.

Söhnel O., Mullin, J.W., (1978). A method for the determination of precipitation induction periods. *Journal of Crystal Growth*, Vol. 44, pp 377- 382.

Ward, J.C., (1970). The structure and properties of some iron sulfides. *Rev. Pure Appl. Chem.*, Vol. 20, pp.175 - 182.